

## Evidence for parallel junctions within high- $T_c$ grain-boundary junctions

E. A. Early, R. L. Steiner, and A. F. Clark

National Institute of Standards and Technology, MET B-258, Gaithersburg, Maryland 20899

K. Char

Conductus, Inc., 969 West Maude Avenue, Sunnyvale, California 94086

(Received 15 September 1993; revised manuscript received 11 April 1994)

Half-integral constant voltage steps were observed in many high- $T_c$  grain-boundary Josephson junctions of  $\text{YBa}_2\text{Cu}_3\text{O}_{7-\delta}$  when a microwave field was applied. Five distinct observed behaviors of the widths of both integral and half-integral steps as a function of microwave amplitude,  $\Delta I_{dc}(I_{ac})$ , are reproduced by simulations of two or three junctions in parallel. This provides quantitative evidence that a single high- $T_c$  grain-boundary junction is composed of several junctions in parallel. These junctions are formed by the overlap of superconducting filaments on either side of the grain boundary, and the spacing between ones with relatively large critical currents is  $\sim 20 \mu\text{m}$ .

### I. INTRODUCTION

We present experimental results on half-integral constant voltage steps in high- $T_c$  grain-boundary junctions. Quantitative comparisons between these results and those obtained by simulations of parallel arrays of junctions enable us to draw conclusions about the microstructure of high- $T_c$  grain-boundary junctions.

One common method for making Josephson junctions in high- $T_c$  materials is to isolate individual grain boundaries.<sup>1-3</sup> There is accumulating evidence that these grain-boundary junctions are inhomogeneous on a microscopic scale. Early results on the magnetic-field dependence of the critical current of such junctions showed a complicated behavior,<sup>4,5</sup> and one particular behavior was well described by assuming a spatially nonuniform junction.<sup>6</sup> A residual critical current even at high magnetic fields<sup>5-9</sup> has been taken as evidence that a grain-boundary junction is composed of a parallel array of junctions. Measurements of  $1/f$  noise are also well described by assuming that there are a number of parallel normal and superconducting connections across a grain boundary.<sup>10,11</sup> Finally, recent electromigration experiments indicate that superconductivity within the bulk film and across a grain boundary is filamentary.<sup>12</sup>

Recently, we observed unusual half-integral constant voltage steps in high- $T_c$   $\text{YBa}_2\text{Cu}_3\text{O}_{7-\delta}$  grain-boundary junctions.<sup>13</sup> A typical current-voltage ( $I$ - $V$ ) curve for such a junction at 4.2 K irradiated with microwaves at a frequency  $\nu \approx 9.3$  GHz is shown in Fig. 1. Note that the curve is symmetric about the origin. To understand this curve, first consider the usual ac Josephson effect.<sup>14</sup> Subjecting a junction to an ac field causes constant voltage steps, also called Shapiro steps,<sup>15</sup> to appear in the  $I$ - $V$  curve. The voltages,  $V$ , of these steps are given by

$$V = n\nu/K_J,$$

where  $n$  is the frequency of the ac field,  $K_J = 2e/h = 0.4835979 \text{ GHz}/\mu\text{V}$  is the Josephson con-

stant, and  $n$  is an integer. Thus, these steps are termed integral steps. For the case shown in Fig. 1, at  $\nu \approx 9.3$  GHz integral steps occur at  $V \approx n \cdot 20 \mu\text{V}$  and are labeled accordingly for positive current polarity. The  $n=0$  step is along the current axis. In addition to these steps, there are distinct steps with voltages given by half-integral  $n$ , e.g., with  $n = \frac{1}{2}, \frac{3}{2}, \frac{5}{2}$ , etc. These are labeled for negative current polarity and are termed half-integral steps.

The concept of step width is important for understanding the results presented in this paper. The step width  $\Delta I_{dc}$  is simply the range of dc current over which the voltage of a step is constant. Thus, for example, the step width of the  $n=2$  step shown in Fig. 1 is approximately  $35 \mu\text{A}$ . The step width is a function of the applied microwave power, and at the microwave power at which the curve in Fig. 1 was obtained, the  $n = \frac{5}{2}$  step is absent.

We have previously proposed that half-integral steps are a result of a single grain-boundary junction actually being composed of many junctions in parallel.<sup>13</sup> We present here more extensive experimental results of the

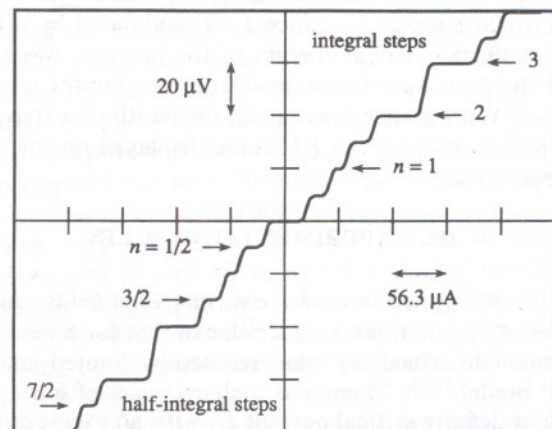


FIG. 1. Current-voltage curve of a 50- $\mu\text{m}$ -wide junction at 4.2 K in a microwave field of 9.3 GHz. Both integral and half-integral steps are indicated by arrows and indexed by  $n$ .

critical currents  $I_{c,j}$  can be unequal, described by  $I_{c,j} = \eta_j I_c$  where the parameter  $\eta_j$  is the fraction of the array critical current carried by junction  $j$ . However, for all junctions  $I_{c,j} R_j = I_c R_n$ . The inductance  $L$  of the loops results in a dimensionless parameter  $\beta_L = 2\pi L I_c / \Phi_0$ , where  $\Phi_0$  is the magnetic flux quanta. The magnetic field within the loops is divided into a normalized applied flux  $f_a = \Phi_a / \Phi_0$  that is uniform across the array and a normalized trapped flux  $f_{t,j}$  within each loop.

Simulation results were obtained by numerically solving the equations that describe the above model using the fourth-order Runge-Kutta method with a step size of  $0.01(2\pi\nu t)$ . Plots of  $\Delta i_{dc}(i_{ac})$  for fixed  $N$ ,  $\Omega$ ,  $\beta_L$ ,  $\eta_j$ ,  $f_a$ , and  $f_{t,j}$  were generated by finding the limits of  $i_{dc}$  for which  $\phi_0 = \sum_j \eta_j \delta_j$  advances by an average of  $2\pi n$  in two ac cycles for a fixed value of  $i_{ac}$ , following a previous suggestion by Belykh, Pedersen, and Soerensen<sup>32</sup> and implementation by Kautz.<sup>33</sup> The width of step  $n$  at that value of  $i_{ac}$  is then the difference between the minimum and maximum values of  $i_{dc}$ , and this procedure is repeated for different values of  $n$  and  $i_{ac}$ . The same technique was used for the dependence of the normalized critical current on normalized magnetic field,  $i_c(f_a)$ , for which  $n=0$ ,  $i_{ac}=0$ , and  $f_a$  is varied.

For the simulation results,  $\Omega=0.175$  was chosen as representative of the experimental values. Using the values in Table I and  $\nu=9.5$  GHz,  $\Omega$  ranges from 0.057 to 0.201, except for one junction with  $\Omega=0.547$ . Also, the simulation results were not sensitively dependent on the value of  $\Omega$ . For two junctions in parallel,  $N=2$ , there is no trapped flux since there is only one loop,  $\eta_0=0.5$  means the junctions were equal, and  $\beta_L=10$  yields good agreement with experimental results and is a reasonable value. For  $N=3$ , all the junctions are equal, the difference in trapped flux between the loops is  $\Delta f_t = f_{t,1} - f_{t,2}$  (where  $f_{t,2} = -f_{t,1}$  for symmetry), and  $\beta_L=15$  for consistency with the results for  $N=2$  since  $\beta_L \propto I_c \propto N$ .

### B. Comparison of experimental and simulation results

For ease of comparison, the experimental results of  $\Delta I_{dc}(I_{ac})$  from Figs. 3(a) to 3(e) are reproduced in Figs. 5(a)–5(e). To the right of each of these figures are selected simulation results of  $\Delta i_{dc}(i_{ac})$ , Figs. 5(f)–5(j). As usual, the panels in each figure correspond, from top to bottom, to the  $n=0, \frac{1}{2}, 1, \frac{3}{2}$ , and 2 steps. For the simulation results, the relevant parameters are given in each figure. Note the excellent agreement between experimental and simulation results in all cases shown in Fig. 5. All the behaviors of  $\Delta I_{dc}(I_{ac})$  for both integral and half-integral steps described and classified in Fig. 3 are reproduced by the simulation results. In addition, there is agreement in nearly all of the finer details of integral step width as a function of ac current amplitude between experiments and simulations. Specifically, experimentally observed nonzero minima of  $\Delta I_{dc}$ , asymmetric shapes of  $\Delta I_{dc}(I_{ac})$ , and even a slight decrease in  $\Delta I_{dc}$  for the  $n=1$  step near

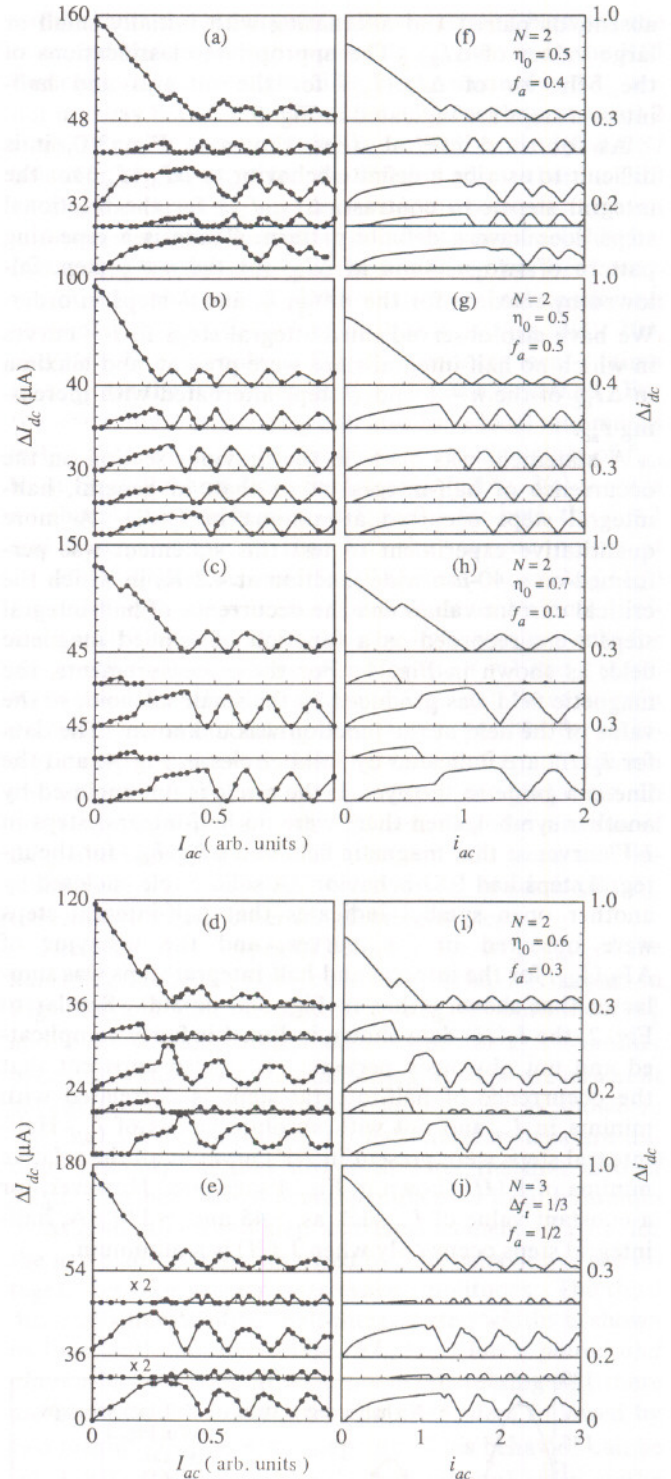


FIG. 5. (a)–(e) Experimental step width  $\Delta I_{dc}$  as a function of microwave amplitude  $I_{ac}$ , reproduced from Fig. 3. (f)–(j) Simulation step width  $\Delta i_{dc}$  as function of ac current amplitude  $i_{ac}$  that reproduces the experimental result shown to the left of the figure. For the simulations, the number of junctions  $N$ , the applied magnetic flux  $f_a$ , the fraction of array critical current carried by the first junction  $\eta_0$  for  $N=2$ , and the difference in trapped magnetic flux between the loops  $\Delta f_t$  for  $N=3$  are indicated. For all simulations  $\Omega=0.175$  and  $\beta_L=10$  for  $N=2$  and 15 for  $N=3$ . In all figures the panels correspond, from top to bottom, to the  $n=0, \frac{1}{2}, 1, \frac{3}{2}$ , and 2 steps.

its first maximum are reproduced in the simulation results. As shown in Fig. 4, half-integral steps occur experimentally at minima of  $I_c(H)$ . Likewise, the simulation results for  $N=2$  shown in Fig. 5 are either close to or at minima of  $i_c(f_a)$ , Fig. 5(f) and Figs. 5(g)–5(i), respectively. Note too that  $\beta_L$  is essentially the only adjustable parameter in the simulations.

A few simulations of  $\Delta i_{dc}(i_{ac})$  for third-integral steps were performed for  $N=3$  with the parameters given above. They did not reproduce the behavior shown in Figs 3(f), although with no trapped flux and  $f_a = \frac{1}{3}$  there were no half-integral steps and the maximum  $\Delta i_{dc}$  of the  $n = \frac{1}{3}$  and  $\frac{2}{3}$  steps alternated with increasing  $i_{ac}$ , which is similar to a behavior we have observed.

### C. Model of grain-boundary junctions

The excellent agreement between experimental and simulation results shown in Fig. 5 is truly remarkable, especially considering that only two or three junctions in parallel are needed. This agreement is direct, quantitative evidence that high- $T_c$  grain-boundary Josephson junctions are actually composed of a parallel array of junctions. It also allows us to propose a microstructural model of grain-boundary junctions.

#### 1. Superconducting filaments

One possible explanation for the ability to reproduce the experimental results with only two junctions in parallel is that grain-boundary junctions could be considered as long. The criteria for a long junction, as opposed to a small one, is that the width of the junction be greater than twice the Josephson penetration depth  $\lambda_J = \sqrt{\hbar/2e\mu_0 d J_c}$ .<sup>14</sup> Here,  $d=2\lambda_L$ , the critical current density of the junction is  $J_c$ , and  $\lambda_L$  is the London penetration depth of the superconductor, which is  $\approx 170$  nm along the  $a$ - $b$  plane of  $\text{YBa}_2\text{Cu}_3\text{O}_{7-\delta}$  at 4.2 K.<sup>20</sup> Using the widths and critical currents listed in Table I,  $\lambda_J$  for all the grain-boundary junctions is on the order of 5  $\mu\text{m}$ . Therefore, all junctions wider than 10  $\mu\text{m}$  could be considered as long. Also, no distinguishing features of long junctions are expected in the  $I$ - $V$  curves of the grain-boundary junctions since overdamped long junctions have  $I$ - $V$  curves that are similar to those of small junctions.<sup>34</sup> With a long junction and an applied magnetic field, the current through the junction is confined to the edges, resulting in two parallel junctions. If this is occurring in these grain-boundary junctions, then all junctions with widths greater than 10  $\mu\text{m}$  should have half-integral steps. However, this is not in agreement with the experimental results shown in Table I, in which all but one of the 20- $\mu\text{m}$ -wide junctions, and even one 50- $\mu\text{m}$ -wide junction, do not have half-integral steps. Also, third-integral steps for  $\Omega=0.175$  result from three junctions in parallel, which implies that in the wider junctions there are more than two junctions in parallel. Thus, these grain-boundary junctions should not be considered as long junctions.

There is an apparent contradiction between the results presented in Fig. 2 and those in Fig. 5. The very compli-

cated and nonperiodic behavior of  $I_c(H)$  implies that there are many junctions in parallel, as suggested by other authors.<sup>5–9</sup> However, the excellent agreement between the experimental and simulation behaviors of  $\Delta I_{dc}(I_{ac})$  implies that there are only two, or at most three, junctions in parallel. The resolution of this apparent contradiction is provided by applying the model of Moeckly, Lathrop, and Buhrman for grain-boundary junctions.<sup>12</sup> In this model, superconductivity in the film is confined to randomly distributed filaments, with transverse dimensions between 1 and 60 nm, that terminate on either side of the grain boundary. Because the transverse dimensions of these filaments are less than the thickness of the film,  $\sim 250$  nm, the ends of the filaments are randomly distributed in the plane of the grain boundary. Overlap of these ends on either side of the grain boundary forms small, weak-link Josephson junctions, with the critical current of each junction being proportional to the area of overlap. Because the distribution of ends in the plane is random, there is a smooth distribution of overlap areas and thus of junction critical currents. This microstructural model for grain-boundary junctions is shown schematically in Fig. 6 for a slice through the grain boundary and parallel to the plane of the substrate. The hatched areas are normal material, with the direction of the  $a$ - $b$  plane indicated on either side of the grain boundary by both the axes and the hatching direction. The superconducting filaments are the clear areas (size exaggerated relative to the normal areas), all with approximately the same size but randomly distributed along both sides of the grain boundary. Thus, as illustrated in Fig. 6, there are some regions along the grain boundary where the overlap of two filaments is small, and other regions where the overlap is large. Consequently, there are many junctions within a grain-boundary junction, a few of which have large critical currents because of large overlap areas. This resolves the apparent contradiction posed above. Many junctions in parallel cause a very complicated behavior of  $I_c(H)$ , but only a few junctions have large critical currents, and these are the ones that determine the behavior of  $\Delta I_{dc}(I_{ac})$  and make it possible to

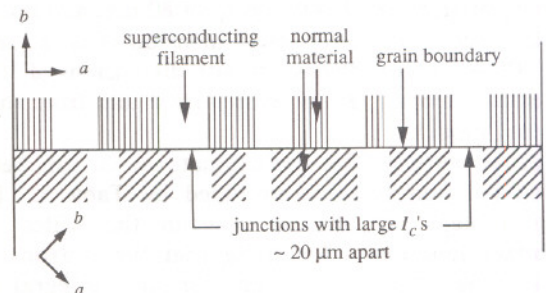


FIG. 6. Schematic representation of a cross section of the microstructure of a grain-boundary junction. Normal material is indicated by hatching, with the alignment of the  $a$ - $b$  planes indicated by both the axes and the hatching direction, while the superconducting filaments are the clear areas (exaggerated size). A junction is formed by the overlap of two filaments on either side of the grain boundary. Junctions formed by large overlaps, and thus with large critical currents, are  $\sim 20$ - $\mu\text{m}$  apart, as discussed in the text.

reproduce this behavior by simulations with only two or three junctions in parallel.

Other consequences of this model are supported by the experimental results. The overlap of filaments across the grain boundary results in weak-link junctions with small capacitances. Such junctions are overdamped, in agreement with nonhysteretic experimental  $I$ - $V$  curves, and further justifies ignoring capacitance in the simulations. The reduction of  $J_c$  in the grain-boundary junctions by a factor of  $10^3$  from its value in the film is consistent with this model. Some of the reduction is due to the depression of the superconducting order parameter at the junction,<sup>35</sup> while the remainder is caused by the failure of many filaments to overlap across the grain boundary. A slight slope of the steps is likely a result of a resistance in parallel with the junctions caused by the overlap of normal areas. Finally, the increase of  $I_c$  with junction width instead of its saturation as reported by Mayer *et al.*<sup>36</sup> is explained by this model. The number of junctions increases with the width of the grain-boundary junction, and thus  $I_c$  also increases with increasing width. There is no saturation because the dimensions of all the parallel junctions are small compared to  $\lambda_J$ .

## 2. Separation between strong junctions

Parallel junctions with relatively large critical currents, here called strong junctions, are indicated to be  $\sim 20 \mu\text{m}$  apart in Fig. 6. This separation distance is based upon the results presented in Table I, where the occurrence of half-integral steps is obviously correlated with the width of the grain-boundary junction. On average, those junctions with widths of  $20 \mu\text{m}$  or less do not have half-integral steps, while those junctions of greater width do. A  $20\text{-}\mu\text{m}$  separation between strong junctions accounts for this correlation. There are, of course, deviations from this because of the random distribution of junctions within a grain boundary. Thus, one  $20\text{-}\mu\text{m}$ -wide junction has half-integral steps while one  $50\text{-}\mu\text{m}$ -wide junction does not. There is also a correlation between the critical current of a junction and the occurrence of half-integral steps, with a cutoff of about  $170 \mu\text{A}$ . Assuming two strong junctions, each with an  $I_c$  of  $80 \mu\text{A}$ , and a bulk  $J_c$  of  $10^7 \text{ A/cm}^2$ , the transverse dimension of each junction is  $\sim 300 \text{ \AA}$ . This is consistent with dimensions of  $10\text{--}600 \text{ \AA}$  deduced from  $I_c(H)$  measurements<sup>8</sup> and from the filamentary model.<sup>12</sup>

Further support for the estimate of  $20 \mu\text{m}$  between strong junctions is again provided by Table I. Third-integral steps are present only in the wider grain-boundary junctions. Assuming that three strong junctions in parallel are necessary for third-integral steps, then on average only the  $50\text{-}\mu\text{m}$ -wide junctions are wide enough to contain three strong junctions. Again, because of the randomness involved with the junctions, one  $40\text{-}\mu\text{m}$ -wide junction has third-integral steps while two  $50\text{-}\mu\text{m}$ -wide junctions do not. Also, the separation between strong junctions can be estimated from the value of  $\beta_L$  used in the simulations. Within a factor of 2,  $\beta_L = 10$  for  $N = 2$  resulted in the best agreement between experimental and simulation results. The inductance of a square

hole in a superconducting film is  $L = (5/4)\mu_0 W$ , where  $W$  is the width of the hole.<sup>37</sup> For a typical  $I_c = 250 \mu\text{A}$  from Table I, the spacing between strong junctions is about  $8 \mu\text{m}$ , which agrees well with the estimate of  $20 \mu\text{m}$  from above considering the approximations used in arriving at this value. This agreement, together with the data in Table I, shows that on average the spacing between strong junctions within a grain boundary is  $20 \mu\text{m}$ . Of course, this estimate is only for grain boundaries with a  $45^\circ$  rotation angle. The spacing could be different for grain boundaries with different rotation angles.

The microstructural model of a single grain-boundary junction being composed of many junctions in parallel, two or three of which have high critical currents, is further supported by simulations of six junctions in parallel. For these simulations,  $\Omega = 0.175$ ,  $\beta_L = 30$ , and 80% of the array critical current was carried by two equal strong junctions separated by one of the four other equal junctions that carried the remainder. The results are shown in Fig. 7, where the array critical current is plotted as a function of applied field in Fig. 7(a), and the step widths are plotted as a function of ac current amplitude in Figs.

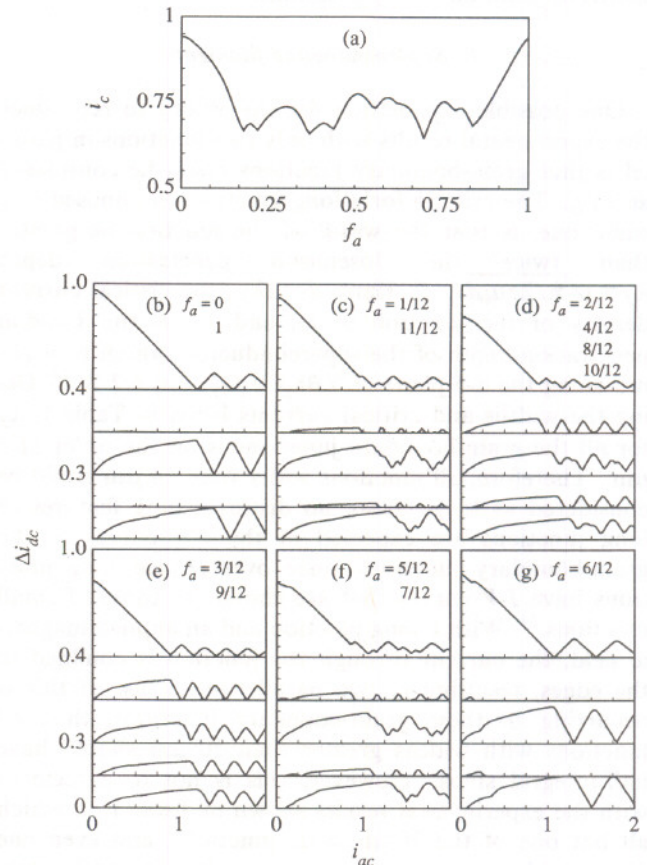


FIG. 7. Simulation results for  $N = 6$ ,  $\Omega = 0.175$ ,  $\beta_L = 30$ , with no trapped flux and with 80% of the array critical current carried by two junctions separated by one of the four equal junctions that carry the remainder of the critical current. (a) Array critical current  $i_c$  as a function of applied magnetic flux  $f_a$ . (b)–(g) Step width  $\Delta i_{dc}$  as a function of ac current amplitude  $i_{ac}$  at the indicated values of  $f_a$ . The panels in each figure correspond, from top to bottom, to the  $n = 0, \frac{1}{2}, 1, \frac{3}{2}$ , and 2 steps.

7(b)–7(g) at the indicated values of applied flux. The behavior of  $i_c(f_a)$  in Fig. 7(a) is complicated with no obvious regular periodicity between  $f_a=0$  and 1, although it is periodic in one flux quanta. This periodicity is present because the parallel array model assumes that the areas of the individual junctions are much less than the areas of the loops formed by the junctions. Thus, there is no Fraunhofer diffraction envelope in  $i_c(f_a)$ . In actual grain-boundary junctions, though, there are numerous parallel junctions of various finite sizes, each contributing a Fraunhofer envelope. This further complicates  $I_c(H)$  and makes direct comparison with simulations of  $i_c(f_a)$  difficult. There is also no symmetry in  $i_c(f_a)$  about  $f_a=\frac{1}{2}$ , although the behavior of  $\Delta i_{dc}(i_{ac})$  is symmetric about  $f_a=\frac{1}{2}$ , as shown in Figs. 7(b)–7(g). These behaviors are similar to those for only two junctions in parallel. Specifically, compare Figs. 7(d) and 5(f), Figs. 7(e) and 5(g), and Figs. 7(g) and 5(h). The behavior shown in Fig. 7(e) is particularly noteworthy. With only two junctions, this behavior is obtained for  $f_a=\frac{1}{2}$ . With six junctions, this same behavior is obtained with  $f_a=\frac{1}{4}$ , which corresponds to half a flux quanta between the two strong junctions. Therefore, these two junctions dominate the behavior of  $\Delta i_{dc}(i_{ac})$  for six junctions in parallel, making it nearly equivalent to that of only two junctions.

### 3. Distribution of parallel junctions

Despite the excellent agreement between experimental and simulation results, actual grain-boundary junctions are likely to be more complicated than the above model suggests. Trapped flux, which depends on the cooldown history of the junction, could change the apparent number of strong junctions in parallel. As an example, the behaviors of  $\Delta I_{dc}(I_{ac})$  shown in Figs. 5(a) and 5(e) were obtained with the same junction but after different cool-downs, and are reproduced with two and three junctions in parallel, respectively. There are also indications that the distribution of critical currents of the parallel junctions within a grain boundary are not random. Assuming a random distribution of equally sized superconducting filaments on each side of the grain boundary, there is an exponential decrease in a histogram of the number of junctions as a function of critical current. Simulations of 16 junctions in parallel with this distribution of critical currents have a noisy behavior of  $\Delta i_{dc}(i_{ac})$  with no correspondence to the behavior of only two junctions in parallel. For the simulations of six junctions in parallel discussed above, the behavior of  $\Delta i_{dc}(i_{ac})$  is like that for two junctions in parallel only if the two strong junctions carry over 70% of the critical current of the array.

Consequently, it seems likely that there are preferred relative critical currents of the parallel junctions. In other words, instead of a monotonic distribution of the number of junctions as a function of critical current, there is a bimodal distribution with many junctions having relatively small critical currents and only a few having much

larger critical currents. One possible mechanism is that there are different types of parallel junctions. If the superconducting filaments occupy a small fraction of the area on each side of the grain boundary, then only a few filaments will overlap across the grain boundary. The few junctions formed in this way could have a much greater critical current than those formed between filaments that were close to each other but did not overlap. Another possibility is that there is some ordering of the filaments within the film. Then, structural models of grain-boundary junctions<sup>38</sup> may be important, as the structure of the grain boundary could favor certain overlap areas of the filaments on either side.

A related consideration is the reproducibility of grain-boundary junctions. The random distribution of filaments assumed in the model presented above implies that junction parameters will have some variability. This is indeed the case experimentally, as shown in Table I, in which different junctions with the same widths have a wide range of parameters. As described in the previous paragraph, there could be some ordering of the filaments at the grain boundary, for example due to the effects of the structure of or stresses within the grain boundary. These effects depend upon the rotation angle of the grain boundary, so at angles other than 45° there may be more or fewer strong junctions, with a corresponding improvement or degradation of reproducibility. Another way to improve the reproducibility of a grain-boundary junction is by increasing its width, thereby increasing the number of strong junctions.

## V. CONCLUSIONS

A variety of experimental behaviors of  $\Delta I_{dc}(I_{ac})$  for both integral and half-integral constant voltage steps in high- $T_c$  grain-boundary junctions were classified. These behaviors were all reproduced by simulations of  $\Delta i_{dc}(i_{ac})$  for two or three junctions in parallel. The excellent agreement between experimental and simulation results provides quantitative evidence that high- $T_c$  grain-boundary junctions are composed of junctions in parallel. The complicated, nonperiodic behavior of  $I_c(H)$  observed experimentally indicates that there are many junctions in parallel. A model of grain-boundary junctions based on superconducting filaments randomly distributed on either side of the grain boundary can explain all the experimental results. The overlap of two filaments on either side of the grain boundary forms a junction, whose critical current is proportional to the area of overlap. Due to the random distribution of filaments, only a few strong junctions are formed. Based on observations of half-integral steps in junctions with various widths, for 45° grain-boundary junctions these strong junctions are  $\sim 20 \mu\text{m}$  apart. The many junctions that are formed in this manner result in a complicated  $I_c(H)$  behavior, while the few strong junctions determine the behavior of  $\Delta I_{dc}(I_{ac})$  for both the integral and half-integral steps. There are

